bioRxiv preprint doi: https://doi.org/10.1101/2025.11.13.688325; this version posted November 14, 2025. The copyright holder for this preprint (which was not certified by peer review) is the author/funder, who has granted bioRxiv a license to display the preprint in perpetuity. It is made available under a CC-BY-NC-ND 4.0 International license.

TrkC has distinct spatiotemporal dynamics compared to TrkA and TrkB

Ryan T. Duffy[1], Stephen J. Hill[1], *Chloe J. Peach[1]

[1]School of Life Sciences, Centre of Membrane Proteins and Receptors (COMPARE), Queen's Medical Centre, Nottingham, UK, NG7 2UH

***Correspondence**: Chloe J. Peach chloe.peach2@nottingham.ac.uk; D19 Medical School, Queen's Medical Centre, Nottingham, NG7 2UH; +44 115 823 0114

bioRxiv preprint doi: https://doi.org/10.1101/2025.11.13.688325; this version posted November 14, 2025. The copyright holder for this preprint (which was not certified by peer review) is the author/funder, who has granted bioRxiv a license to display the preprint in perpetuity. It is made available under a CC-BY-NC-ND 4.0 International license.

Abstract

Neurotrophins are critical regulators of neuronal development and have been implicated as therapeutic targets in a range of neurodegenerative and psychiatric disorders. Nerve growth factor (NGF), brain-derived neurotrophic factor (BDNF), neurotrophin-3 (NT-3), and neurotrophin-4 (NT-4) signal through the receptor tyrosine kinase family of tropomyosin receptor kinase (Trk) receptors. These include TrkA responding to canonical ligand NGF, TrkB responding to BDNF or NT-4, and TrkC responding to NT-3. While TrkA and TrkB have been comparatively well studied, the fundamental pharmacological properties of TrkC remain largely unexplored. Here, we developed and utilised real-time bioluminescence- or fluorescence-based resonance energy transfer (BRET or FRET) biosensors to study the real-time spatial and temporal dynamics at 37°C to profile Trk receptor dimerisation, trafficking and nuclear ERK signalling in response to neurotrophin stimulation. TrkA and TrkB displayed consistent concentration-dependent dimerisation, trafficking, and signalling. TrkC, on the other hand, exhibited considerable dimerisation but reduced trafficking and ERK signalling relative to TrkA or TrkB. There was also evidence for comparable activation by both canonical and some non-canonical ligands across the Trk family in response to NGF, BDNF, NT-3, or NT-4 across signalling and trafficking assays. The divergence between robust receptor oligomerisation and minimal trafficking suggests TrkC is subject to unique molecular mechanisms distinct from TrkA or TrkB.

bioRxiv preprint doi: https://doi.org/10.1101/2025.11.13.688325; this version posted November 14, 2025. The copyright holder for this preprint (which was not certified by peer review) is the author/funder, who has granted bioRxiv a license to display the preprint in perpetuity. It is made available under a CC-BY-NC-ND 4.0 International license.

Introduction

Neurotrophins are a highly conserved family of growth factors that are critical for the development and maintenance of the nervous system (Huang & Reichardt, 2001). Nerve growth factor (NGF) was first identified through its ability to promote the survival and outgrowth of peripheral neurons (Levi-Montalcini & Angeletti, 1963), where subsequent studies led to the identification of additional neurotrophic growth factors including brain-derived neurotrophic factor (BDNF; Barde et al., 1982), neurotrophin-3 (NT-3; Hohn et al., 1990), and neurotrophin-4/5 (NT-4; Hallbook et al., 1991).

Neurotrophins signal through the tropomyosin receptor kinase (Trk) family of receptor tyrosine kinases (RTKs), comprising TrkA, TrkB and TrkC, for which the canonical ligands are NGF/TrkA (Klein et al., 1991; Wiesmann et al., 1999), BDNF/TrkB, NT-4/TrkB TrkB (Naylor et al., 2002) and NT-3/TrkC (Urfer et al., 1994). Growth factor stimulation promotes receptor dimerisation and the auto- and transphosphorylation of key intracellular tyrosine residues. This enables the recruitment of key intracellular adaptor proteins, initiating downstream signalling cascades such as mitogen-activated protein kinase (MAPK/ERK), phosphoinositide 3-kinase (PI3K/AKT) and phospholipase Cγ signalling pathways (Mitre et al., 2017). Together, these signalling events coordinate a range of neuronal processes including survival, synaptic plasticity and circuit refinement (Ohira & Hayashi, 2009).

Following ligand binding and signal transduction, Trk receptors undergo receptor endocytosis in a clathrin-dependent manner (Zheng et al., 2008), which enables retrograde transport along axons to specific subcellular compartments (Harrington & Ginty, 2013). From these intracellular endosomes, there is extensive evidence that TrkA (Grimes et al., 1997; Howe et al., 2001) and TrkB (Moya-Alvarado et al., 2023) can continue to signal. Despite our understanding of the role of Trk receptors in physiology (Deinhardt & Chao, 2014), there are limited direct comparisons between the isolated pharmacology of TrkA, TrkB and TrkC with spatial and temporal resolution, at least in-part due to high homology between Trk subtypes and the neurotrophic ligands that activate multiple Trk receptors.

To monitor real-time Trk receptor pharmacology in an isolated system, resonance energy transfer-based approaches such as bioluminescence resonance energy transfer (BRET) and fluorescence resonance energy transfer (FRET) can be utilised (Stoddart et al., 2018). These techniques rely on the transfer of energy from a donor molecule to an acceptor molecule when within close proximity (<10 nm), allowing the quantitative analysis of protein-protein interactions with temporal resolution at 37°C. Building on our previous studies across RTKs

bioRxiv preprint doi: https://doi.org/10.1101/2025.11.13.688325; this version posted November 14, 2025. The copyright holder for this preprint (which was not certified by peer review) is the author/funder, who has granted bioRxiv a license to display the preprint in perpetuity. It is made available under a CC-BY-NC-ND 4.0 International license.

(Peach et al., 2021; Peach et al., 2024), we aimed to develop and utilise these real-time assays to systematically characterise the real-time pharmacology of TrkA, TrkB, and TrkC. By directly comparing their dimerisation, subcellular trafficking and downstream ERK signalling induced in response to NGF, BDNF, NT-3 and NT-4, we identified both shared and notably divergent features of Trk receptor dynamics, particularly with respect to TrkC.

Methods

Cell Culture and materials

HEK293T cells were cultured using Dulbecco's Modified Eagle Medium (DMEM) containing 10% foetal bovine serum (FBS) (Sigma Aldrich, US) and 1% penicillin streptomycin antibiotic (Sigma Aldrich, US). HEK293T cells were incubated at 37°C in a humidified incubator with 5% CO_2. Cells were monitored daily and were split using a ratio of 1:10 or 1:15 to maintain a suitable growth confluency. Once cells reached 90% confluency, HEK293T cells were seeded at a density of 25,000 cells per well in a standard 96-well white clear bottom plate (#655089, Greiner Bio-One) for BRET experiments. For FRET, a standard 96-well black clear bottom plate (#G655209, Greiner Bio-One) was used. Hanks' Balanced Salt Solution (HBSS), with calcium and glucose was purchased from Thermo Fisher Scientific (#14025092). HEPES buffer (H23830), Bovine Serum Albumin (A9418), and Phorbol 12,13-dilbutyrate (PDBu) (P1269) were all purchased from Sigma Aldrich. Furimazine was bought from Promega Corporation (N1110). SNAP-Surface Alexa Fluor 488 was bought from (New England Biolabs, S9129S). All neurotrophic growth factors were bought from Alomone Labs, including NGF (#N-245), BDNF (#B-250), NT-3 (#N-260), and NT-4 (#N-270). Coelenterazine Purple was bought from NanoLight technology (#369-1). Polyethyleneimine (PEI) was purchased from Polysciences (24765).

Generating DNA Constructs

N-terminal NanoLuc-tagged and SnapTag-tagged TrkA, (NM_001012331), TrkB (NM_006180), and TrkC (NM_002530) were generated in the pFN28K expression vector. Each construct included the IL-6 signal peptide fused to the N-terminus of either nanoluciferase (NanoLuc) or SnapTag respectively, followed by a GSSGAIA linker and the coding sequence of the respective Trk receptor. C-terminal *Renilla* luciferase (Rluc8)-tagged

bioRxiv preprint doi: https://doi.org/10.1101/2025.11.13.688325; this version posted November 14, 2025. The copyright holder for this preprint (which was not certified by peer review) is the author/funder, who has granted bioRxiv a license to display the preprint in perpetuity. It is made available under a CC-BY-NC-ND 4.0 International license.

TrkA, TrkB, and TrkC were cloned in pcDNA5 vector encoding the full length Trk receptor, followed by a HA-tag (YPYDVPDYA), and then the Rluc8 sequence.

DNA Transfections

For all studies, following 24h, HEK293T cells were serum starved prior to transfection using DMEM without serum supplementation to remove growth factors in FBS. Cells were then transfected with transfection reagent polyethyleneimine (PEI)) at ratio of 1:6 ratio DNA to PEI. Cells were incubated for 48 hours to allow the expression prior to assays.

To quantify trafficking, HEK293T cells were transfected with each Trk receptor tagged on the C-terminus with Rluc8 either TrkA-HA-Rluc8, TrkB-HA-Rluc8, or TrkC-HA-Rluc8 (20ng/well), as well as a marker of the plasma membrane tagged with Renilla green fluorescent protein (RGFP), RGFP-CAAX (20 ng/well). To quantify dimerisation, HEK293T cells were transfected with DNA encoding Trk receptors tagged on the N-terminus with a NanoLuc (NanoLuc-Trk, 10 ng/well) and a SnapTag (SnapTag-Trk, 25 ng/well). To quantify ERK signalling, HEK293T cells were transfected with nuclear EKAR CFP YFP (40 ng/well; Addgene, #18681) and N-terminal SnapTag-Trk (20 ng/well).

Dimerisation BRET Assay

HEK293T cells were transfected with DNA encoding Trk receptors tagged at the N-terminus with either a luminescent donor, NanoLuc, or a SnapTag. Following 48h serum starvation and transfection, cells were incubated with SNAP-Surface Alexa Fluor 488 to label receptor at the plasma membrane. Cells were pre-incubated with SnapTag (0.25 μM, 1 hour) at 37°C. Cells were then washed in assay buffer to remove unbound substrate. Cells were incubated with furimazine (NanoLuc substrate; 600X dilution) for 5 minutes at 37°C. BRET was measured using the PHERAstar FSX microplate reader (BMG Labtech). Following 5 baseline reads, ligand was added at increasing concentrations (1pM-30nM). The plate was then read every 45 seconds for a further 20 minutes using a BRET1 plus filter (donor wavelength of 475 nm and acceptor wavelength 535 nm). BRET ratios were calculated by dividing the emission intensity of the acceptor wavelength by the donor wavelength emission intensity, thus providing a ratiometric change in BRET.

bioRxiv preprint doi: https://doi.org/10.1101/2025.11.13.688325; this version posted November 14, 2025. The copyright holder for this preprint (which was not certified by peer review) is the author/funder, who has granted bioRxiv a license to display the preprint in perpetuity. It is made available under a CC-BY-NC-ND 4.0 International license.

Trafficking BRET Assay

All assays used HBSS with calcium and glucose (#14025092 Thermo Fisher Scientific, US) supplemented with HEPES buffer (pH 7.4) with 0.1% Bovine Serum Albumin (BSA). Following 48h serum starvation and transfection, assay buffer was added to each well, followed by Coelenterazine Purple (BRET substrate for Rluc8; 400X dilution). Each plate was incubated at 37°C for 5 minutes to allow the enzymatic reaction to occur. BRET reads were measured in the PHERAstar FSX microplate reader (BMG Labtech) using a BRET2 filter, (donor wavelength of 370–450 nm and acceptor wavelength 500–540 nm). Following 5 baseline reads, increasing concentrations (1 pM-30 nM) of NGF, BDNF, NT-3 or NT-4 were added. The plate was then read every 74 seconds for a further 25 minutes. BRET ratios were calculated as explained in the dimerisation assay.

Nuclear ERK FRET Assays

On the day of the assay 48h post-transfection, cells were incubated in assay buffer and left to incubate for at least 30 minutes before stimulating with increasing agonist concentrations of NGF, BDNF, NT-3 or NT-4 (0.1 pM-30 nM). Phorbol 12,13-dibutyrate (PDBu, 10 µM) was used as a positive control and the buffer solution was used as a vehicle treatment. FRET reads were measured in the PHERAstar microplate reader (BMG Labtech) using a “FI 430 530 480” optic module. Donor excitation was provided at 430 nm (CFP), donor emission was recorded at 480 nm, and acceptor emission (YFP) was recorded at 530 nm following donor excitation. Following 5 baseline reads, increasing concentrations (1 pM-30 nM) of NGF, BDNF, NT-3 or NT-4 were added. The plate was then read every 63 seconds for a further 20 minutes. FRET ratio was calculated as ratio (530nm/480nm) of the two emission signals.

Data Analysis

Data were analysed using GraphPad Prism (10.1.2). Data were baseline-corrected to the 5 reads prior to ligand addition, then baseline-corrected to changes in vehicle over time. For ERK signalling, data were then normalised to the maximal response of the positive control (PDBu, 100%), expressed as a percentage relative to vehicle (0%). Concentration-response data were fit using non-linear regression analysis as log vs. response (three parameters) **“Y=Bottom + (Top-Bottom)/(1+10^(LogEC50-X))”** to determine EC_{50} values. Concentration–response curves from the Trk trafficking assay were inverted to represent receptor endocytosis

bioRxiv preprint doi: https://doi.org/10.1101/2025.11.13.688325; this version posted November 14, 2025. The copyright holder for this preprint (which was not certified by peer review) is the author/funder, who has granted bioRxiv a license to display the preprint in perpetuity. It is made available under a CC-BY-NC-ND 4.0 International license.

driven by growth factor agonism. To compare kinetic values, data from experiments using 30 nM NGF, BDNF, NT-3, and NT-4 were analysed by non-linear regression using a one-phase association model: **"$Y = Y_0 + (Plateau - Y_0)(1 - e^{-Kx})$"** to determine Kobs. Data points prior to 0 minutes were excluded, as no ligand had been added at that time. For ERK signalling specifically, data between 2 and 15 minutes were used to ensure an appropriate kinetic fit that captured a single association phase. Significance was determined on concentration-response data using ordinary two-way ANOVA followed by Dunnett's multiple comparisons test, with all experimental groups compared to vehicle ($\alpha = 0.05$). Significance was accepted at $p<0.05$ (*), $p<0.01$ (**), $p<0.001$ (***), and $p<0.0001$ (****).

Results

Development of a Trk dimerisation assay

To investigate Trk receptor dimerisation, we developed a BRET-based assay to measure the proximity of Trk monomers following ligand stimulation. To facilitate this, a NanoLuciferase (NanoLuc, luminescent donor) and SnapTag (fluorescent acceptor) were tagged on the N-terminus of each monomer (*Figure 1A*). We first assessed the effect of canonical ligands for each Trk subtypes on their real-time dimerisation in response to increasing concentrations of neurotrophin (*Figure 1B-E*). At their cognate Trk receptor, each ligand induced a robust increase in the BRET ratio in a concentration-dependent manner. NGF-induced TrkA dimerisation and both BDNF- and NT-4-induced TrkB dimerisation demonstrated similar changes in the BRET ratio (*Figure 1B-D*). TrkC, on the other hand, had a more pronounced increase in the BRET ratio in response to NT-3 compared to TrkA or TrkB (*Figure 1E*). Due to these distinct canonical ligands, it is unknown whether this effect is driven by NT-3 or by an intrinsic property of the TrkC receptor.

TrkC demonstrates atypical dimerisation compared to TrkA and TrkB

To probe whether these distinctions in dimerisation are ligand-associated or receptor-associated, we monitored Trk receptor dimerisation in response to both canonical and non-canonical ligands. Dimerisation of TrkA was induced by NGF, as well as NT-4, but not in response to BDNF (*Figure 2A*). Due to this concentration-dependent response, the BRET ratio following ~20-minute stimulation was plotted as a concentration-response curve (*Figure 2B*).

bioRxiv preprint doi: https://doi.org/10.1101/2025.11.13.688325; this version posted November 14, 2025. The copyright holder for this preprint (which was not certified by peer review) is the author/funder, who has granted bioRxiv a license to display the preprint in perpetuity. It is made available under a CC-BY-NC-ND 4.0 International license.

Quantifying the potency of neurotrophin-induced TrkA dimerisation (pEC_{50}, *Table 1*), NGF had an EC_{50} 1.32 nM while the potency of TrkA dimerisation was comparable for NT-3 and NT-4. As well as deriving the potency for each neurotrophin, we used these real-time methods to quantify the kinetic parameters of neurotrophin-induced dimerisation (K_{obs}; *Table 1)*.

TrkB dimerisation was observed in response to BDNF, NT-3, and NT-4 (*Figure 2C*). This rapid and robust increase in BRET ratio was concentration-dependent (*Figure 2D*). NT-4 was the most potent at inducing dimerisation of TrkB dimerisation (EC_{50} 0.6 nM). BDNF and NT-3 provided similar potencies (EC_{50} 1.9 - 2.6 nM; *Table 1*). NGF, however, did not induce any significant change in BRET ratio throughout the duration of the experiment.

A large TrkC dimerisation response was induced by both NT-3 and BDNF (*Figure 2E*). This was concentration-dependent (*Figure 2F*), where the potency for NT-3 (EC_{50} ~2 nM) was 20X higher than that of BDNF with respect to TrkC dimerisation (*Table 1*). Both NGF and NT-4, on the other hand, failed to induce any change in BRET ratio for TrkC dimerisation (*Figure 2E,F*).

<u>Comparing real-time trafficking across the Trk family</u>

Given the pronounced change in BRET during the TrkC dimerisation assay, the next objective was to compare across the trafficking of Trk receptors in real-time. To achieve this, a BRET-based assay was established tagging the C-terminus with Rluc8 and using a RGFP-CAAX as a plasma membrane marker (*Figure 3A*). Upon ligand stimulation, receptor internalisation leads to trafficking away from the plasma membrane and the RGFP-CAAX marker, meaning a decrease in BRET ratio. In response to increasing concentrations of its canonical ligand, there was trafficking of Trk receptors away from the plasma membrane marker with a sustained reduction in BRET signal (*Figure 3B-E*).

This was then compared across Trk receptors, selectively isolating the movement of tagged Trk subtypes away from the plasma membrane. Concentration-response curves (*Figure 4B,D,E*) were generated from baseline-corrected BRET ratio at ≈ 20-minutes of the corresponding kinetic graphs (*Figure 3B-E*). From these data, the potency of ligand-induced trafficking (pEC_{50}; *Table 2*), and kinetic parameters (K_{obs}; *Table 2*) were derived to quantify difference across Trk receptors. TrkA trafficking was most potently induced by NGF (EC_{50} 0.95 nM; *Table 2*), with NT-3 and NT-4 eliciting less potent responses (EC_{50} 14.8 nM and 6.92 nM respectively; *Table 2*). BDNF was unable to induce this extent of TrkA trafficking (*Figure 4A*). TrkB trafficking was similar in the sense that all ligands induced a measurable change in BRET,

bioRxiv preprint doi: https://doi.org/10.1101/2025.11.13.688325; this version posted November 14, 2025. The copyright holder for this preprint (which was not certified by peer review) is the author/funder, who has granted bioRxiv a license to display the preprint in perpetuity. It is made available under a CC-BY-NC-ND 4.0 International license.

with canonical BDNF being the most potent (EC_{50} 2.34 nM; *Table 2*) and NGF being the least potent (EC_{50} 8.91 nM), whilst NGF only induced a partial trafficking response compared to the other growth factors (*Figure 4C*). NT-3 and NT-4 induced a similar TrkB trafficking response with potencies of 3.31 nM and 3.39 nM respectively (*Table 2*).

In comparison to TrkA and TrkB, the trafficking of TrkC was diminished across all ligand concentrations. Only NT-3 induced a noticeable reduction in BRET in a concentration-dependent manner at physiologically-relevant concentrations (*Figure 3E; Table 2;* EC_{50} 0.45 nM). This was reduced compared to how TrkA and TrkB traffic away from the plasma membrane (*Figure 4 A,C,E*). NGF and NT-4, on the other hand, were able to induce TrkC trafficking (*Figure 4E*).

Minimal ERK signalling in response to TrkC

To determine the downstream consequences of ligand stimulation, we then used a FRET-based assay to assess the level of ERK phosphorylation following ligand stimulation. An EKAR sensor localised to the nucleus was used due its proximity to transcriptional events, enabling live-cell detection of ERK activity within this defined subcellular compartment (*Figure 5A*). When ERK is activated, it phosphorylates the substrate domain on EKAR; this induces a conformational change that brings the donor and acceptor fluorophores into close proximity, inducing an increase in FRET (Harvey et al., 2008). Phorbol 12,13-dibutyrate (PDBu) was used as a positive control as a potent activator of protein kinase C, thus leading to ERK activation (Bapat et al., 2001). Stimulation with canonical ligands induced robust ERK signalling in cells expressing TrkA and TrkB, reflected by a large increase in the FRET ratio (*Figure 5B-D*). In contrast, NT-3-induced ERK activation *via* TrkC was minimal, even at 30 nM (*Figure 5E*).

We next investigated real-time ERK signalling in response to all neurotrophins (*Figure 6*). Concentration-response curves were also generated from the baseline-corrected FRET ratio (*Figure 6 B,D,F)* to quantify the potency of ligand-induced nuclear ERK signalling was generated (pEC_{50}*; Table 3*), as well as kinetic parameters (K_{obs}*; Table 3*). ERK signalling downstream of TrkA was detected in response to all neurotrophic growth factors, with NGF producing the strongest and most potent change in the FRET ratio (EC_{50} ~0.12 nM; *Table 3*). BDNF induced an ERK response at TrkA at concentrations exceeding 10 nM, therefore no EC_{50} could be calculated from this concentration range (*Figure 6B*). TrkB showed a comparable response profile to TrkA, with BDNF, NT-3, and NT-4 all inducing clear,

bioRxiv preprint doi: https://doi.org/10.1101/2025.11.13.688325; this version posted November 14, 2025. The copyright holder for this preprint (which was not certified by peer review) is the author/funder, who has granted bioRxiv a license to display the preprint in perpetuity. It is made available under a CC-BY-NC-ND 4.0 International license.

concentration-dependent ERK activation (*Figure 6B, E*). While BDNF, NT-3, and NT-4 all showed high potency at TrkB, NT-4 was the most potent (EC_{50} ~0.06 nM) at inducing ERK signalling *via* TrkB (*Table 3*). NGF stimulation of TrkB only led to a modest increase in FRET; similarly to BDNF-induced ERK signalling at TrkA, partial NGF ERK signalling at TrkB was only detectable at concentrations exceeding 10 nM.

In contrast, TrkC-expressing HEK293T cells were less responsive to neurotrophic ligands with respect to ERK signalling. NT-3 elicited a measurable increase in the FRET ratio that was concentration-dependent (*Figure 5E*). Although weak, NT-3 induced a potent TrkC-mediated nuclear ERK response (EC_{50} 0.87 nM), reaching a peak of ~40% of positive control PDBu. In terms of kinetics, TrkC-mediated ERK activation was also delayed, with an ERK response only beginning after 5 minutes with a peak after 10 minutes (*Figure 6E)*, even at the highest NT-3 concentration at the top of the concentration-response curve. This was slower than ERK signalling in response to TrkA and TrkB, which saw an increase in ERK activation after 3 minutes and peaked in <10 minutes after addition of their canonical ligand (*Figure 5 A,C*) or non-canonical ligands (*Figure 6 A,C*). Both TrkA and TrkB ERK signalling declined after the 10-minute peak, whereas TrkC maintained its partial ERK activity for the remainder of the assay, further highlighting the unique nature of TrkC.

Discussion

Our study demonstrates that TrkC has markedly distinct spatial and temporal characteristics compared to TrkA and TrkB. While TrkC had reduced receptor trafficking relative to TrkA and TrkB, there was an enhanced degree of RTK dimerisation. Accordingly, TrkC also exhibited a lower extent of nuclear ERK signalling relative to TrkA or TrkB. Establishing these approaches with spatial and temporal resolution enabled not only direct comparisons across neurotrophins, but also to isolate the defined pharmacology of each human Trk subtype expressed in isolation. These distinct spatial and temporal dynamics at human TrkC were apparent even in response to the same ligand – the promiscuous neurotrophin, NT-3 – demonstrating unique pharmacological properties as a mechanism inherent to TrkC.

Compared to TrkA and TrkB, there was reduced internalisation observed for TrkC. Accordingly, whereas it is well-established that TrkA (Howe et al., 2001) and TrkB (Zheng et al., 2008) undergo clathrin-mediated endocytosis and continue to signal from these increasingly acidic subcellular endosomes (Bhattacharyya et al., 1997; Harrington et al., 2011; Philippidou et al.,

bioRxiv preprint doi: https://doi.org/10.1101/2025.11.13.688325; this version posted November 14, 2025. The copyright holder for this preprint (which was not certified by peer review) is the author/funder, who has granted bioRxiv a license to display the preprint in perpetuity. It is made available under a CC-BY-NC-ND 4.0 International license.

2011), TrkC endocytosis is less well-characterised. This is in-part due to the limitations of a TrkC-selective ligand, where our data support that BDNF and NT-3 can activate both TrkB and TrkC. With neurons in the central nervous system often co-expressing TrkB and TrkC (Kokaia et al., 1995; Ateaque et al., 2022), the ability to delineate TrkC-specific pharmacology is difficult in endogenously expressing systems. There is evidence, however, for TrkC endocytosis in response to NT-3 in retinal ganglion cells, suggesting a distinct trafficking route *via* the Golgi apparatus (Butowt & Von Bartheld, 2001). Accordingly, we also observed a slower movement of TrkC away from the GFP-tagged plasma membrane marker upon NT-3 stimulation, which may link to the translocation of TrkC to distinct subcellular compartments.

Consistent with these distinct spatial dynamics, we also observed notably slower and reduced overall ERK signalling downstream of TrkC activation, relative to TrkA and TrkB. That said, we did detect a concentration-dependent NT-3 response, in agreement with studies measuring TrkC-induced ERK signalling (Li et al., 2016; Brahimi et al., 2021; Ateaque et al., 2022). We also derived a potency of 0.9 nM for NT-3-induced ERK signalling, comparable to the NT-3/TrkC potency derived using Western blotting against phosphorylated ERK (Szobota et al., 2019; EC_{50} 0.4 nM). This extent of the maximum NT-3-induced ERK response, however, was only ~40% of that observed for TrkA and TrkB. Given the aforementioned importance of endosomal signalling in the Trk family, we propose that this could link to the limited degree of TrkC trafficking observed. In accordance with this, we detected real-time ERK using a nuclear EKAR sensor due to its proximity to the subcellular location that leads to the subsequent transcriptional changes. While this downstream sensor is likely to detect signalling from both the plasma membrane and from subcellular compartments, this could account for the 5-10 minute delay observed for the peak ERK response at TrkC, even at the highest NT-3 concentration. This real-time approach therefore reveals that despite having relatively similar potencies across TrkA, TrkB and TrkC, the resulting ERK signalling in response to NT-3 at TrkC was markedly slower – an effect likely to be even more pronounced in neurons that require long-range retrograde transport of signalling endosomes along the axon to reach the nucleus in the cell body.

Interestingly, the inverse was observed with regards to the extent of TrkC dimerisation, whereby neurotrophin stimulation led to considerably greater TrkC dimerisation compared to TrkA and TrkB. One explanation could be attributed to the extent of dimerisation prior to the addition of neurotrophins. There is evidence that TrkA and TrkB – akin to other RTKs – can exist as inactive, pre-formed dimers at the plasma membrane under resting conditions (Shen & Maruyama, 2011; Shen & Maruyama, 2012). This was later shown for TrkC (Ahmed & Hristova, 2018), however if there were fewer pre-formed TrkC dimers relative to TrkA/TrkB in

bioRxiv preprint doi: https://doi.org/10.1101/2025.11.13.688325; this version posted November 14, 2025. The copyright holder for this preprint (which was not certified by peer review) is the author/funder, who has granted bioRxiv a license to display the preprint in perpetuity. It is made available under a CC-BY-NC-ND 4.0 International license.

this specific cellular microenvironment, this could lead to a larger change in BRET upon the formation of a dimeric – or even oligomeric – homomeric complex. A second explanation could relate to the nature of BRET measuring close proximity between two tags. As such, as well as representing two monomers forming a dimer, increased BRET could also denote a dramatic conformational re-arrangement upon ligand stimulation. This was also suggested in a study measuring FRET between C-terminally tagged Trk receptors (Ahmed & Hristova, 2018), suggesting a distinct conformational rearrangement of TrkC. A third explanation could link to evidence of TrkC acting as a 'dependence receptor' that, in the absence of ligand, can contrastingly lead to cell death (Tauszig-Delamasure et al., 2007). If there was caspase-mediated cleavage of the intracellular portion of TrkC, this could lead to a disconnect between the ability for TrkC to dimerise at the plasma membrane, yet reducing receptor endocytosis or downstream ERK signalling. That said, upon overexpression in the absence of ligand, cells expressing TrkC did not undergo noticeable cell death. There is also evidence that TrkA can act as a dependence receptor (Nikoletopoulou et al., 2010), thus not accounting for the TrkC-specific differences across receptor dimerisation, internalisation and ERK signalling relative to TrkA/TrkB. It is likely, however, that a reduced extent of TrkC endocytosis would enable a greater degree of receptor dimerisation at the cell surface. While we do not see a transient dimerisation response for readily internalising TrkA or TrkB, the increasingly acidic microenvironment of intracellular endosomes may affect the BRET signal between Trk homodimers.

While Trk receptors are paired with their 'canonical' neurotrophins, our findings provide definitive evidence for additional 'non-canonical' pairings. Supporting other studies showing cross-family signalling (Ivanisevic et al., 2007), this demonstrates both potencies and kinetics that were sometimes comparable between canonical and non-canonical ligands. Both NT-4 and NT-3, for example, induced TrkA dimerisation with a similar potency to NGF. In the context of TrkB, 'promiscious' NT-3 robustly stimulated TrkB dimerisation, trafficking and signalling, showing dynamics comparable to BDNF and NT-4. Confirming the selectivity of these novel assays, however, NGF failed to induce TrkB dimerisation and produced weak endocytosis. There were broader distinctions observed between canonical and non-canonical ligands with respect to ERK signalling. This could be in-part linked to signal amplification of the downstream ERK assay. Furthermore, NGF elicited a modest ERK response *via* TrkB, despite limited lacking significant dimerisation or trafficking. This was also observed with BDNF-induced TrkA ERK signalling, despite neither ligand, nor NT-4, inducing an ERK response in cells expressing TrkC. Delineating these distinctions required the selectivity of these approaches for tagged receptors alone, something particularly critical for the Trk receptor family given their high degree of homology.

bioRxiv preprint doi: https://doi.org/10.1101/2025.11.13.688325; this version posted November 14, 2025. The copyright holder for this preprint (which was not certified by peer review) is the author/funder, who has granted bioRxiv a license to display the preprint in perpetuity. It is made available under a CC-BY-NC-ND 4.0 International license.

It should also be noted that our *in vitro* model strategically lacks some key co-receptors implicated in Trk receptor biology. Although HEK293T cells likely express sortilin, a Trk co-receptor shown to regulate TrkC trafficking (Vaegter et al., 2011; Klein et al., 2023), HEK293T notably lack $p75^{NTR}$ (Conroy & Coulson, 2022; Peach et al., 2024) and express minimal NGF/TrkA modulator neuropilin-1 (Peach et al., 2024). These kinetic approaches not only enable high-throughput drug screening for Trk agonists or antagonists at the human receptor (*e.g.*, *de novo* designed NGF mimetics (Schlichthaerle et al., 2025)), but these spatiotemporal methods provide a model to systematically interrogate the distinct roles of how co-receptors modulate Trk dimerisation, trafficking and signalling kinetics in real-time.

In conclusion, TrkC displayed a distinct pharmacological profile compared to TrkA and TrkB, showing robust ligand-induced dimerisation, but reduced trafficking and ERK signalling. Given the therapeutics interest in targeting Trk receptors across a range of neurodegenerative diseases (Mansoor et al., 2024) and psychiatric disorders (Kim et al., 2024), understanding the molecular mechanisms by which these receptors compare and contrast will guide future efforts to develop drugs targeting the appropriate spatial and temporal properties for the preferred Trk subtype. Furthermore, despite notably high homology across the Trk family, this study demonstrates a nuanced model of Trk receptor dynamics with mechanistic distinctions across their signalling and trafficking.

bioRxiv preprint doi: https://doi.org/10.1101/2025.11.13.688325; this version posted November 14, 2025. The copyright holder for this preprint (which was not certified by peer review) is the author/funder, who has granted bioRxiv a license to display the preprint in perpetuity. It is made available under a CC-BY-NC-ND 4.0 International license.

References

Hohn A., Leibrock J., Bailey K., & Barde Y.A. (1990). Identification and characterization of a novel member of the nerve growth factor/brain-derived neurotrophic factor family. *Nature*, 344(6264), 339-41. https://doi.org/10.1038/344339a0

Ahmed, F., & Hristova, K. (2018). Dimerization of the Trk receptors in the plasma membrane: Effects of their cognate ligands. *Biochemical Journal*, *475*(22), 3669–3685. https://doi.org/10.1042/BCJ20180637

Ateaque, S., Merkouris, S., Wyatt, S., Allen, N. D., Xie, J., DiStefano, P. S., Lindsay, R. M., & Barde, Y. A. (2022). Selective activation and down-regulation of Trk receptors by neurotrophins in human neurons co-expressing TrkB and TrkC. *Journal of Neurochemistry*, *161*(6), 463–477. https://doi.org/10.1111/jnc.15617

Bapat, S., Verkleij, A., & Post, J. A. (2001). Peroxynitrite activates mitogen-activated protein kinase (MAPK) via a MEK-independent pathway: A role for protein kinase C. *FEBS Letters*, *499*(1–2), 21–26. https://doi.org/10.1016/S0014-5793(01)02511-X

Barde, Y.A., Edgar, D., & Thoenen, H. (1982). Purification of a new neurotrophic factor from mammalian brain. *EMBO Journal* 1(5), 549-53. https://doi.org/10.1002/j.1460-2075.1982.tb01207.x

Bhattacharyya, A., Watson, F. L., Bradlee, T. A., Pomeroy, S. L., Stiles, C. D., & Segal, R. A. (1997). Trk Receptors Function As Rapid Retrograde Signal Carriers in the Adult Nervous System. *J Neurosci*. 17(18), 7007-16. https://doi.org/10.1523/jneurosci.17-18-07007.1997

Brahimi F., Galan A., Siegel S., Szobota S., Sarunic M. V., Foster A. C., Saragovi H. U. (2021). Therapeutic Neuroprotection by an Engineered Neurotrophin that Selectively Activates Tropomyosin Receptor Kinase (Trk) Family Neurotrophin Receptors but Not the p75 Neurotrophin Receptor. *Mol Pharmacol*. 100(5):491-501. doi: 10.1124/molpharm.121.000301.

Butowt, R., & Von Bartheld, C. S. (2001). Sorting of Internalized Neurotrophins into an Endocytic Transcytosis Pathway via the Golgi System: Ultrastructural Analysis in

bioRxiv preprint doi: https://doi.org/10.1101/2025.11.13.688325; this version posted November 14, 2025. The copyright holder for this preprint (which was not certified by peer review) is the author/funder, who has granted bioRxiv a license to display the preprint in perpetuity. It is made available under a CC-BY-NC-ND 4.0 International license.

Retinal Ganglion Cells. *J Neurosci.* 21(22), 8915-30. https://doi.org/10.1523/jneurosci.21-22-08915.2001

Conroy, J. N., & Coulson, E. J. (2022). High-affinity TrkA and p75 neurotrophin receptor complexes: A twisted affair. *The Journal of Biological Chemistry*, *298*(3), 101568. https://doi.org/10.1016/j.jbc.2022.101568

Deinhardt, K., & Chao, M. V. (2014). Trk Receptors. *Handbook Experimental Pharamcology.* 220:103-19. https://doi.org/10.1007/978-3-642-45106-5_5

Grimes, M. L., Beattie, E., & Mobley, W. C. (1997). A signaling organelle containing the nerve growth factor-activated receptor tyrosine kinase, TrkA. *Proceedings of the National Academy of Sciences of the United States of America*, *94*(18), 9909–9914. https://doi.org/10.1073/pnas.94.18.9909

Hallbook, F., Ibanez, C. F., & Persson, H. (1991). Evolutionary Studies of the Nerve Growth Factor Family Reveal a Novel Member Abundantly Expressed in Xenopus Ovary. *Neuron* 6(5) 845-58. https://doi.org/10.1016/0896-6273(91)90180-8

Harrington, A. W., & Ginty, D. D. (2013). Long-distance retrograde neurotrophic factor signalling in neurons. *Nature Reviews Neuroscience* 14(3) 177–18). https://doi.org/10.1038/nrn3253

Harrington, A. W., St. Hillaire, C., Zweifel, L. S., Glebova, N. O., Philippidou, P., Halegoua, S., & Ginty, D. D. (2011). Recruitment of actin modifiers to TrkA endosomes governs retrograde NGF signaling and survival. *Cell*, 146(3), 421–434. https://doi.org/10.1016/j.cell.2011.07.008

Harvey, C. D., Ehrhardt, A. G., Cellurale, C., Zhong, H., Yasuda, R., Davis, R. J., Svoboda, K. (2008). A genetically encoded fluorescent sensor of ERK activity. *Proceedings of the National Academy of Sciences of the United States of America*, 105(49), 19264-9. https://doi.org/10.1073/pnas.0804598105

He, L., & Hristova, K. (2012). Physical–chemical principles underlying RTK activation, and their implications for human disease. *Biochimica et Biophysica Acta (BBA) - Biomembranes*, *1818*(4), 995–1005. https://doi.org/https://doi.org/10.1016/j.bbamem.2011.07.044

bioRxiv preprint doi: https://doi.org/10.1101/2025.11.13.688325; this version posted November 14, 2025. The copyright holder for this preprint (which was not certified by peer review) is the author/funder, who has granted bioRxiv a license to display the preprint in perpetuity. It is made available under a CC-BY-NC-ND 4.0 International license.

Howe, C. L., Valletta, J. S., Rusnak, A. S., & Mobley, W. C. (2001). NGF Signaling from Clathrin-Coated Vesicles: Evidence that Signaling Endosomes Serve as a Platform for the Ras-MAPK Pathway. *Neuron*. 32(5), 801-14. https://doi.org/10.1016/s0896-6273(01)00526-8

Huang, E. J., & Reichardt, L. F. (2001). Neurotrophins: Roles in neuronal development and function. *Annual Review of Neuroscience* 24, 677–736. https://doi.org/10.1146/annurev.neuro.24.1.677

Ivanisevic, L., Zheng, W. H., Woo, S. B., Neet, K. E., & Saragovi, H. U. (2007). TrkA receptor “hot spots” for binding of NT-3 as a heterologous ligand. *Journal of Biological Chemistry*, *282*(23), 16754–16763. https://doi.org/10.1074/jbc.M701996200

Kim, J., He, M. J., Widmann, A. K., & Lee, F. S. (2024). The role of neurotrophic factors in novel, rapid psychiatric treatments. *Neuropsychopharmacology*, 49(1), 227–245. https://doi.org/10.1038/s41386-023-01717-x

Klein, R., Jing, S. Q., Nanduri, V., O'Rourke, E., & Barbacid, M. (1991). The trk proto-oncogene encodes a receptor for nerve growth factor. *Cell*, *65*(1), 189–197. https://doi.org/10.1016/0092-8674(91)90419-y

Klein, M., Failla, A. V., & Hermey, G. (2023). Internally tagged Vps10p-domain receptors reveal uptake of the neurotrophin BDNF. *Journal of Biological Chemistry*, *299*(10). https://doi.org/10.1016/j.jbc.2023.105216

Kokaia Z., Metsis M., Kokaia M., Elmér E., Lindvall O. (1995). Co-expression of TrkB and TrkC receptors in CNS neurones suggests regulation by multiple neurotrophins. *Neuroreport*. 6(5):769-72. doi: 10.1097/00001756-199503270-00016

Levi-Montalcini R, & Angeletti PU. (1963). Essential role of the nerve growth factor in the survival and maintenance of dissociated sensory and sympathetic embryonic nerve cells in vitro. *Developmental Biology*, 6, 653–659. https://doi.org/10.1016/0012-1606(63)90149-0

Li, R., Wu, Y., & Jiang, D. (2016). NT-3 attenuates the growth of human neuron cells through the ERK pathway. *Cytotechnology*, *68*(4), 659–664. https://doi.org/10.1007/s10616-014-9813-1

bioRxiv preprint doi: https://doi.org/10.1101/2025.11.13.688325; this version posted November 14, 2025. The copyright holder for this preprint (which was not certified by peer review) is the author/funder, who has granted bioRxiv a license to display the preprint in perpetuity. It is made available under a CC-BY-NC-ND 4.0 International license.

Mansoor, S., Jindal, A., Badu, N. Y. A., Katiki, C., Ponnapalli, V. J. S., Desai, K. J., & Nassar, S. T. (2024). Role of Neurotrophins in the Development and Treatment of Neurodegenerative Diseases: A Systematic Review. *Cureus*, 16(11), e74048. https://doi.org/10.7759/cureus.74048

Merkouris, S., Barde, Y. A., Binley, K. E., Allen, N. D., Stepanov, A. V, Wu, N. C., Grande, G., Lin, C.-W., Li, M., Nan, X., Chacon-Fernandez, P., DiStefano, P. S., Lindsay, R. M., Lerner, R. A., & Xie, J. (2018). Fully human agonist antibodies to TrkB using autocrine cell-based selection from a combinatorial antibody library. *Proceedings of the National Academy of Sciences of the United States of America*, 115(30), E7023–E7032. https://doi.org/10.1073/pnas.1806660115

Mitre, M., Mariga, A., & Chao, M. V. (2017). Neurotrophin signalling: Novel insights into mechanisms and pathophysiology. *Clinical Science (London)* 131(1), 13–23. https://doi.org/10.1042/CS20160044

Moya-Alvarado, G., Tiburcio-Felix, R., Ibáñez, M. R., Aguirre-Soto, A. A., Guerra, M. V, Wu, C., Mobley, W. C., Perlson, E., & Bronfman, F. C. (2023). BDNF/TrkB signaling endosomes in axons coordinate CREB/mTOR activation and protein synthesis in the cell body to induce dendritic growth in cortical neurons. *eLife*, *12:e77455*. https://doi.org/10.7554/eLife.77455

Naylor, R. L., Robertson, A. G. S., Allen, S. J., Mason, G. G. F., Burston, J. J., Tyler, S. J., Dawbarn, D., Sessions, R. B., Clarke, A. R., & Wilcock, G. K. (2002). A discrete domain of the human TrkB receptor defines the binding sites for BDNF and NT-4. *Biochemical and Biophysical Research Communications*, *291*(3), 501–507. https://doi.org/10.1006/bbrc.2002.6468

Nikoletopoulou, V., Lickert, H., Frade, J. M., Rencurel, C., Giallonardo, P., Zhang, L., Bibel, M., & Barde, Y.-A. (2010). Neurotrophin receptors TrkA and TrkC cause neuronal death whereas TrkB does not. *Nature*, *467*(7311), 59–63. https://doi.org/10.1038/nature09336

Ohira, K., & Hayashi, M. (2009). A New Aspect of the TrkB Signaling Pathway in Neural Plasticity. *Current Neuropharmacology*. 7(4) 276-85. https://doi.org/10.2174/157015909790031210

bioRxiv preprint doi: https://doi.org/10.1101/2025.11.13.688325; this version posted November 14, 2025. The copyright holder for this preprint (which was not certified by peer review) is the author/funder, who has granted bioRxiv a license to display the preprint in perpetuity. It is made available under a CC-BY-NC-ND 4.0 International license.

1 Peach, C.J., Kilpatrick, L. E., Woolard, J., & Hill, S. J. (2021). Use of NanoBiT and
2 NanoBRET to monitor fluorescent VEGF-A binding kinetics to VEGFR2/NRP1
3 heteromeric complexes in living cells. *British Journal of Pharmacology*, *178*(12), 2393–
4 2411. https://doi.org/10.1111/bph.15426

5 Peach C. J., Tonello R., Damo E., Gomez K., Calderon-Rivera A., Bruni R., Bansia H.,
6 Maile L., Manu A. M., Hahn H., Thomsen A. R., Schmidt B. L., Davidson S., des Georges
7 A., Khanna R., & Bunnett N. W. (2024). Neuropilin-1 inhibition suppresses nerve growth
8 factor signaling and nociception in pain models. *Journal of Clinical Investigation*.
9 135(4):e183873. https://doi.org/10.1172/jci183873

10 Philippidou, P., Valdez, G., Akmentin, W., Bowers, W. J., Federoff, H. J., & Halegoua, S.
11 (2011). Trk retrograde signaling requires persistent, Pincher-directed endosomes.
12 *Proceedings of the National Academy of Sciences of the United States of America*,
13 *108*(2), 852–857. https://doi.org/10.1073/pnas.1015981108

14 Schlichthaerle, T., Yang, A., Detraux, D., Johnson, D. E., Peach, C. J., Edman, N. I.,
15 Sniezek, C., Williams, C. A., Arora, S., Katiyar, N., Chen, I., Etemadi, A., Favor, A., Lee,
16 D., Kubo, C., Coventry, B., Huang, B., Gerben, S., Ennist, N., … Baker, D. (2025).
17 Designed NGF mimetics with reduced nociceptive signatures in neurons. *BioRxiv*,
18 2025.04.14.648806. https://doi.org/10.1101/2025.04.14.648806

19 Shen, J., & Maruyama, I. N. (2011). Nerve growth factor receptor TrkA exists as a
20 preformed, yet inactive, dimer in living cells. *FEBS Letters*, *585*(2), 295–299.
21 https://doi.org/10.1016/j.febslet.2010.12.031

22 Shen, J., & Maruyama, I. N. (2012). Brain-derived neurotrophic factor receptor TrkB
23 exists as a preformed dimer in living cells. *Journal of Molecular Signaling*, 7(1).
24 https://doi.org/10.1186/1750-2187-7-2

25 Stoddart, L. A., Kilpatrick, L. E., & Hill, S. J. (2018). NanoBRET Approaches to Study
26 Ligand Binding to GPCRs and RTKs. *Trends in Pharmacological Sciences*, *39*(2), 136–
27 147. https://doi.org/10.1016/j.tips.2017.10.006

28 Szobota, S., Mathur, P. D., Siegel, S., Black, K. A., Uri Saragovi, H., & Foster, A. C.
29 (2019). BDNF, NT-3 and Trk receptor agonist monoclonal antibodies promote neuron
30 survival, neurite extension, and synapse restoration in rat cochlea ex vivo models

bioRxiv preprint doi: https://doi.org/10.1101/2025.11.13.688325; this version posted November 14, 2025. The copyright holder for this preprint (which was not certified by peer review) is the author/funder, who has granted bioRxiv a license to display the preprint in perpetuity. It is made available under a CC-BY-NC-ND 4.0 International license.

relevant for hidden hearing loss. *PLoS ONE*, *14*(10). https://doi.org/10.1371/journal.pone.0224022

Tauszig-Delamasure, S., Yu, L.-Y., Cabrera, J. R., Bouzas-Rodriguez, J., Mermet-Bouvier, C., Guix, C., Bordeaux, M.-C., Arumäe, U., & Mehlen, P. (2007). The TrkC receptor induces apoptosis when the dependence receptor notion meets the neurotrophin paradigm. *Proceedings of the National Academy of Sciences of the United States of America*, *104*(33), 13361–13366. https://doi.org/10.1073/pnas.0701243104

Urfer, R., Tsoulfas, P., Soppet, D., Escandon, E., Parada, L. F., & Presta, L. G. (1994). The binding epitopes of neurotrophin-3 to its receptors trkC and gp75 and the design of a multifunctional human neurotrophin. *EMBO Journal,* 13(24), 5896-909. https://doi.org/10.1002/j.1460-2075.1994.tb06935.x

Vaegter, C. B., Jansen, P., Fjorback, A. W., Glerup, S., Skeldal, S., Kjolby, M., Richner, M., Erdmann, B., Nyengaard, J. R., Tessarollo, L., Lewin, G. R., Willnow, T. E., Chao, M. V., & Nykjaer, A. (2011). Sortilin associates with Trk receptors to enhance anterograde transport and neurotrophin signaling. *Nature Neuroscience*, *14*(1), 54–63. https://doi.org/10.1038/nn.2689

Wiesmann, C., Ultsch, M. H., Bass, S. H., & de Vos, A. M. (1999). Crystal structure of nerve growth factor in complex with the ligand-binding domain of the TrkA receptor. *Nature*, *401*, 184–188.

Zheng, J., Shen, W. H., Lu, T. J., Zhou, Y., Chen, Q., Wang, Z., Xiang, T., Zhu, Y. C., Zhang, C., Duan, S., & Xiong, Z. Q. (2008a). Clathrin-dependent endocytosis is required for TrkB-dependent Akt-mediated neuronal protection and dendritic growth. *Journal of Biological Chemistry*, *283*(19), 13280–13288. https://doi.org/10.1074/jbc.M709930200

bioRxiv preprint doi: https://doi.org/10.1101/2025.11.13.688325; this version posted November 14, 2025. The copyright holder for this preprint (which was not certified by peer review) is the author/funder, who has granted bioRxiv a license to display the preprint in perpetuity. It is made available under a CC-BY-NC-ND 4.0 International license.

Figures & Figure Legends

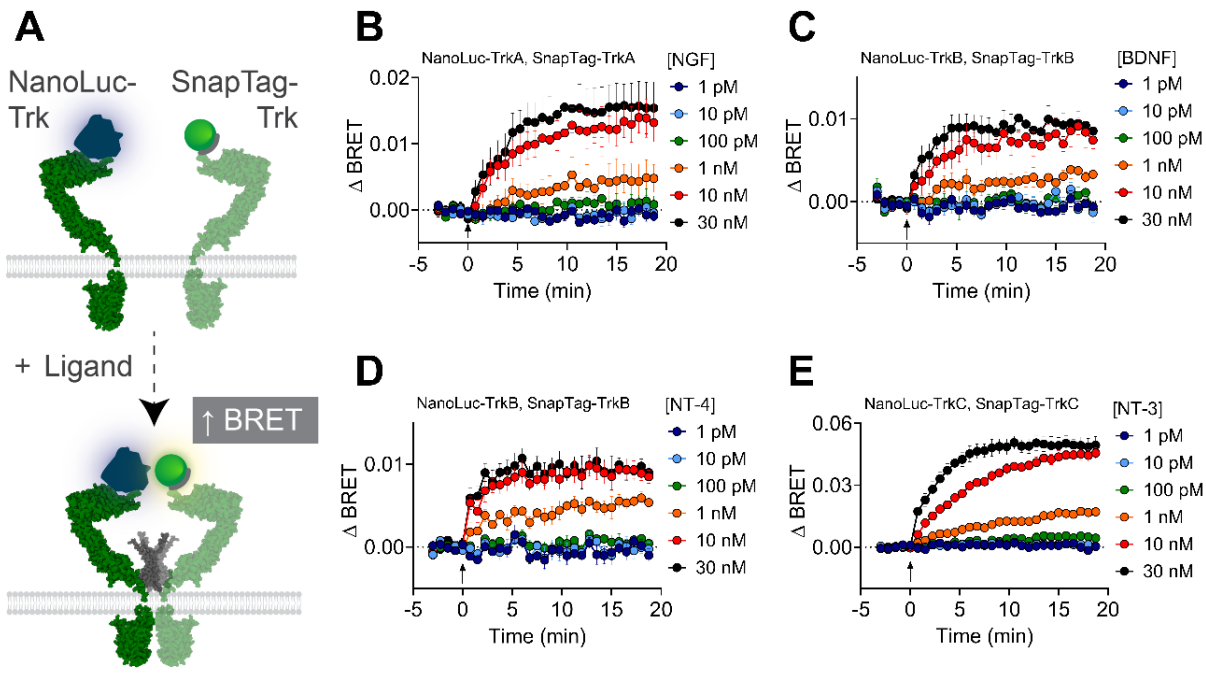


Figure 1. **Developing a real-time assay monitoring Trk dimerisation in response to canonical neurotrophin ligands**. (A) Schematic of the dimerisation assay measuring bioluminescence resonance energy transfer (BRET) between the luminescent donor enzyme (NanoLuc) and fluorescent acceptor (SnapTag-AlexaFluor488). (B-E) HEK293T cells expressing NanoLuc- and SnapTag-labelled TrkA (B), TrkB (C,D) or TrkC (E) were stimulated with increasing growth factor concentrations at T=0 (arrow). Data are expressed as the change in BRET ratio over time. Mean ± SEM, from 4-5 independent experiments with triplicate wells.

bioRxiv preprint doi: https://doi.org/10.1101/2025.11.13.688325; this version posted November 14, 2025. The copyright holder for this preprint (which was not certified by peer review) is the author/funder, who has granted bioRxiv a license to display the preprint in perpetuity. It is made available under a CC-BY-NC-ND 4.0 International license.

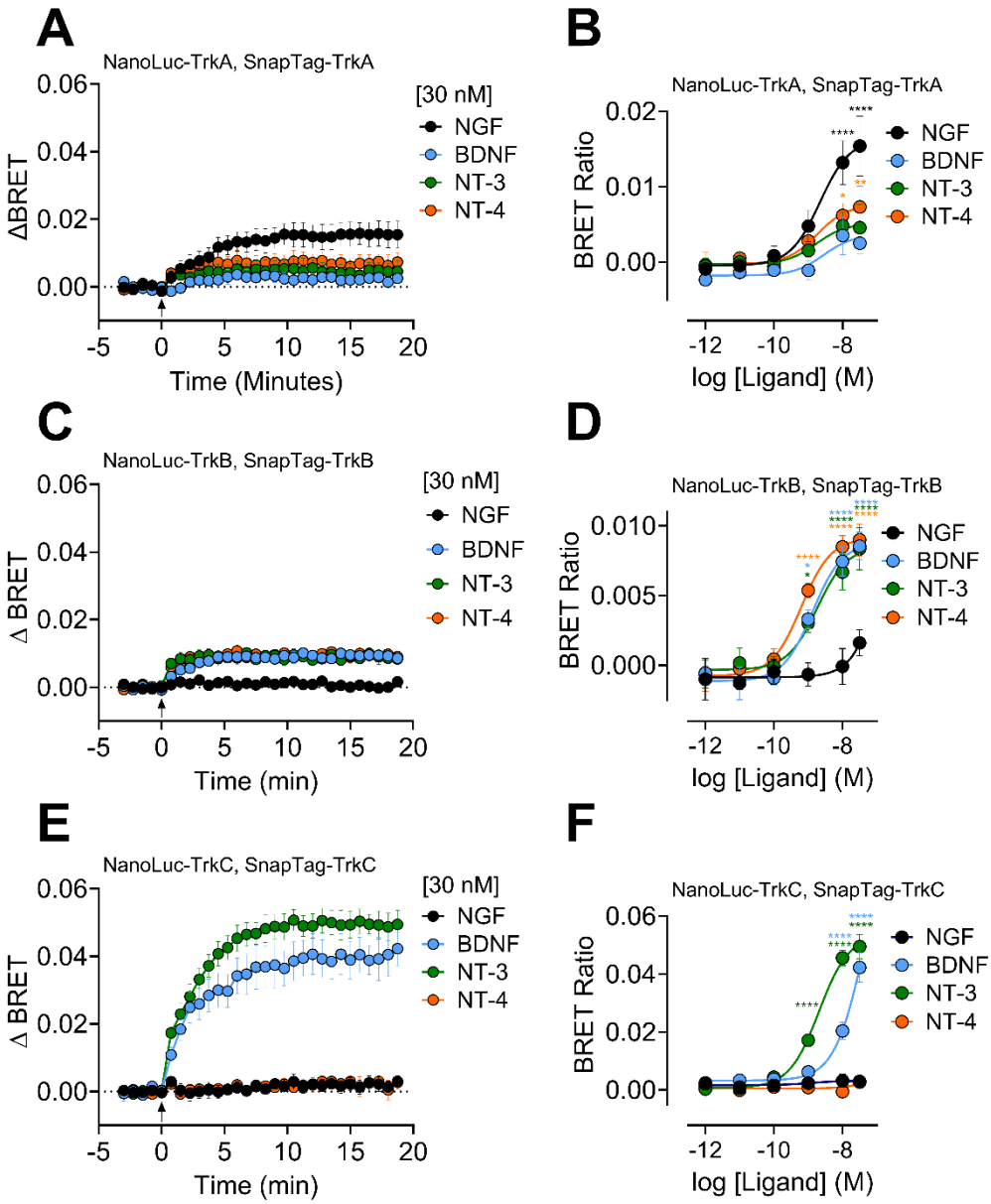


Figure 2: **Concentration-dependent dimerisation of TrkA, TrkB and TrkC across the neurotrophin family.** (A,C,E) Dimerisation between TrkA, TrkB or TrkC for all four neurotrophins (30 nM), including the top concentration of canonical ligand from Fig.1. (B,D,F) Concentration-response across a range of concentrations plotting the baseline-corrected BRET ratio from ~20 minutes. Mean ± SEM, from 4-5 independent experiments with triplicate wells. Potency values (pEC_{50}, Table 1) and kinetic parameters (k_{obs}, Table 1) were fit using a non-linear regression. Significance (B,D,F) was determined using ordinary two-way ANOVA with Dunnett's multiple comparisons test versus vehicle. Statistical significance denoted as p<0.05 (*), p<0.01 (**), p<0.001 (***), and p<0.0001 (****).

bioRxiv preprint doi: https://doi.org/10.1101/2025.11.13.688325; this version posted November 14, 2025. The copyright holder for this preprint (which was not certified by peer review) is the author/funder, who has granted bioRxiv a license to display the preprint in perpetuity. It is made available under a CC-BY-NC-ND 4.0 International license.

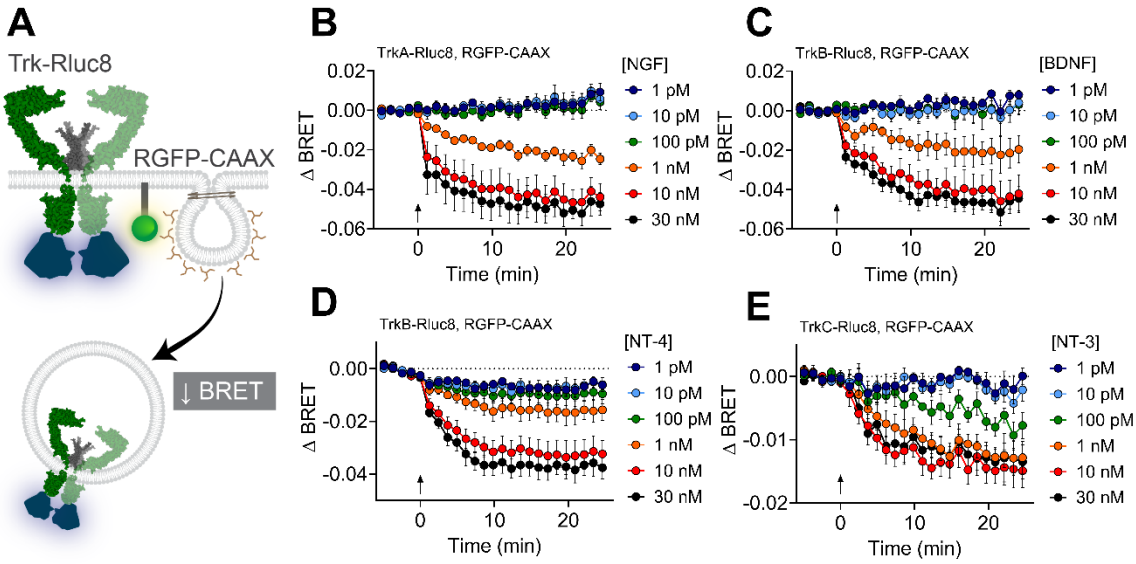


Figure 3. **Monitoring Trk trafficking in real-time in response to canonical neurotrophin ligands.** (A) Schematic of the Trk trafficking assay measuring BRET between Trk-HA-Rluc8 (bioluminescent donor) and RGFP-CAAX (fluorescent acceptor). (B-E) Trafficking interactions away from the plasma membrane in response to canonical growth factors. Data are expressed as change in BRET ratio over 25 minutes n=5. Ligand (1 pM - 30 nM) was added at T=0 (arrow). Data points represent mean ± SEM, from 5 independent experiments with triplicate wells.

bioRxiv preprint doi: https://doi.org/10.1101/2025.11.13.688325; this version posted November 14, 2025. The copyright holder for this preprint (which was not certified by peer review) is the author/funder, who has granted bioRxiv a license to display the preprint in perpetuity. It is made available under a CC-BY-NC-ND 4.0 International license.

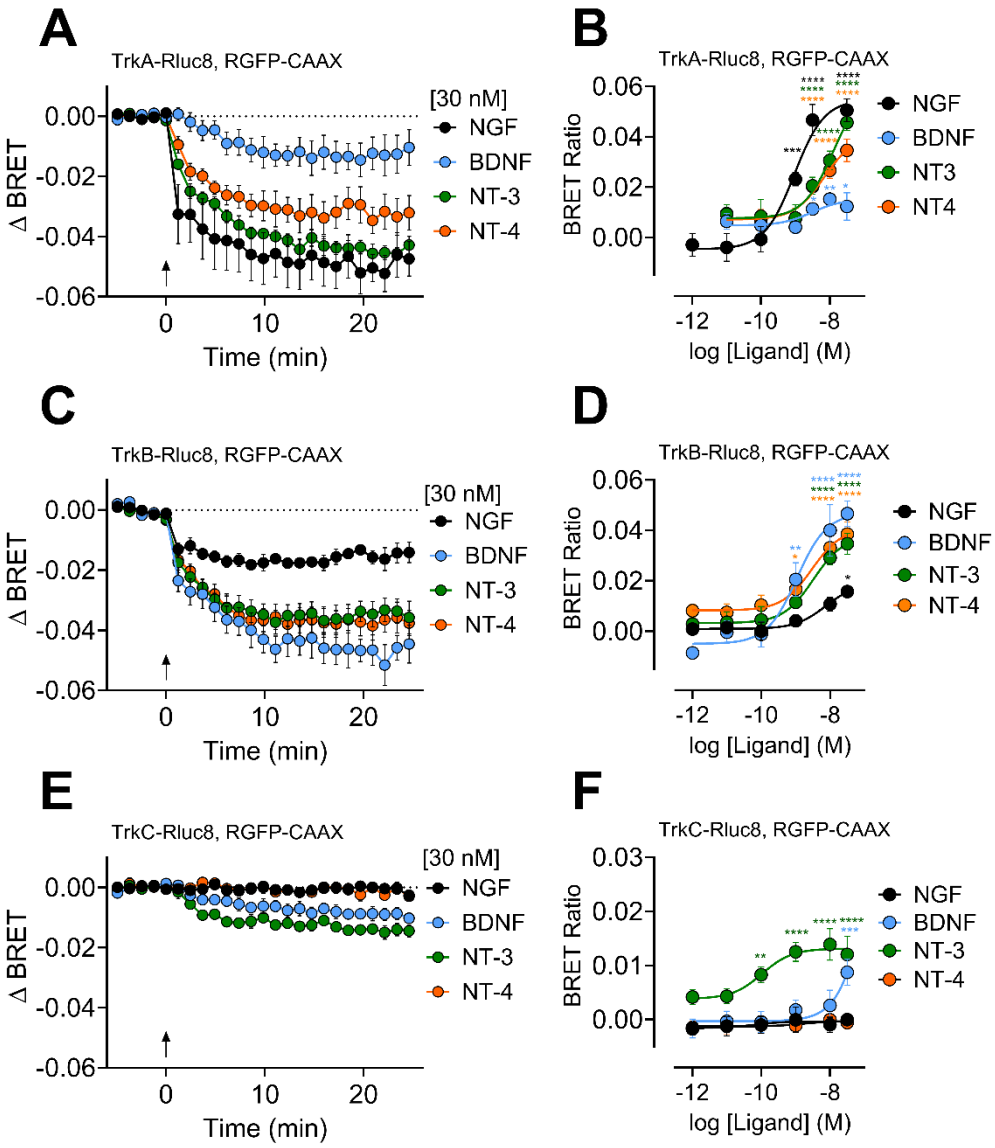


Figure 4. **TrkC had reduced trafficking away from the plasma membrane marker compared to TrkA or TrkB.** (A,C,E) Trafficking in response to 30 nM of each neurotropic growth factors. Data are expressed as change in BRET ratio over 25 minutes. (B,D,F) Concentration–response curves were generated from the baseline-corrected BRET ratio at ≈20 min of the corresponding kinetic graphs (Fig. 3B–E) and inverted to reflect growth factor–induced receptor endocytosis. Mean ± SEM, from 5 independent experiments with triplicate wells. Derived potency and kinetic values are provided in Table 2. Significance (D,F) was determined using ordinary two-way ANOVA with Dunnett's multiple comparisons test versus vehicle. Statistical significance denoted as p<0.05 (*), p<0.01 (**), p<0.001 (***), and p<0.0001(****).

bioRxiv preprint doi: https://doi.org/10.1101/2025.11.13.688325; this version posted November 14, 2025. The copyright holder for this preprint (which was not certified by peer review) is the author/funder, who has granted bioRxiv a license to display the preprint in perpetuity. It is made available under a CC-BY-NC-ND 4.0 International license.

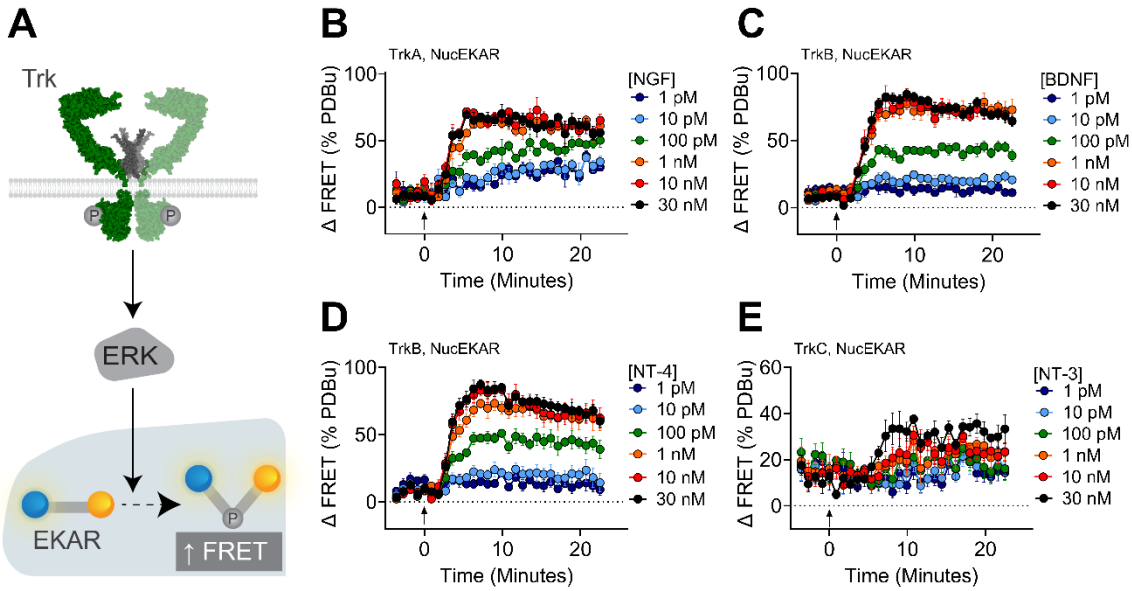


Figure 5. **Neurotrophin-induced ERK signalling kinetics**. (A) Trk-mediated ERK signalling leads to activation of nuclear ERK sensor, a sensor based on fluorescence resonance energy transfer (FRET). (B-E) HEK293T cells expressed SnapTag-TrkA, SnapTag-TrkB or SnapTag-TrkC, where the SnapTag was not conjugated to a fluorophore. Cells were stimulated with increasing growth factor concentrations (1 pM - 30nM) at T=0 (arrow). Data expressed as change in FRET ratio over 25 minutes and expressed as a percentage of vehicle (0%) and 10 μM PDBu (100%). Mean ± SEM, from 4-5 independent experiments with triplicate wells.

bioRxiv preprint doi: https://doi.org/10.1101/2025.11.13.688325; this version posted November 14, 2025. The copyright holder for this preprint (which was not certified by peer review) is the author/funder, who has granted bioRxiv a license to display the preprint in perpetuity. It is made available under a CC-BY-NC-ND 4.0 International license.

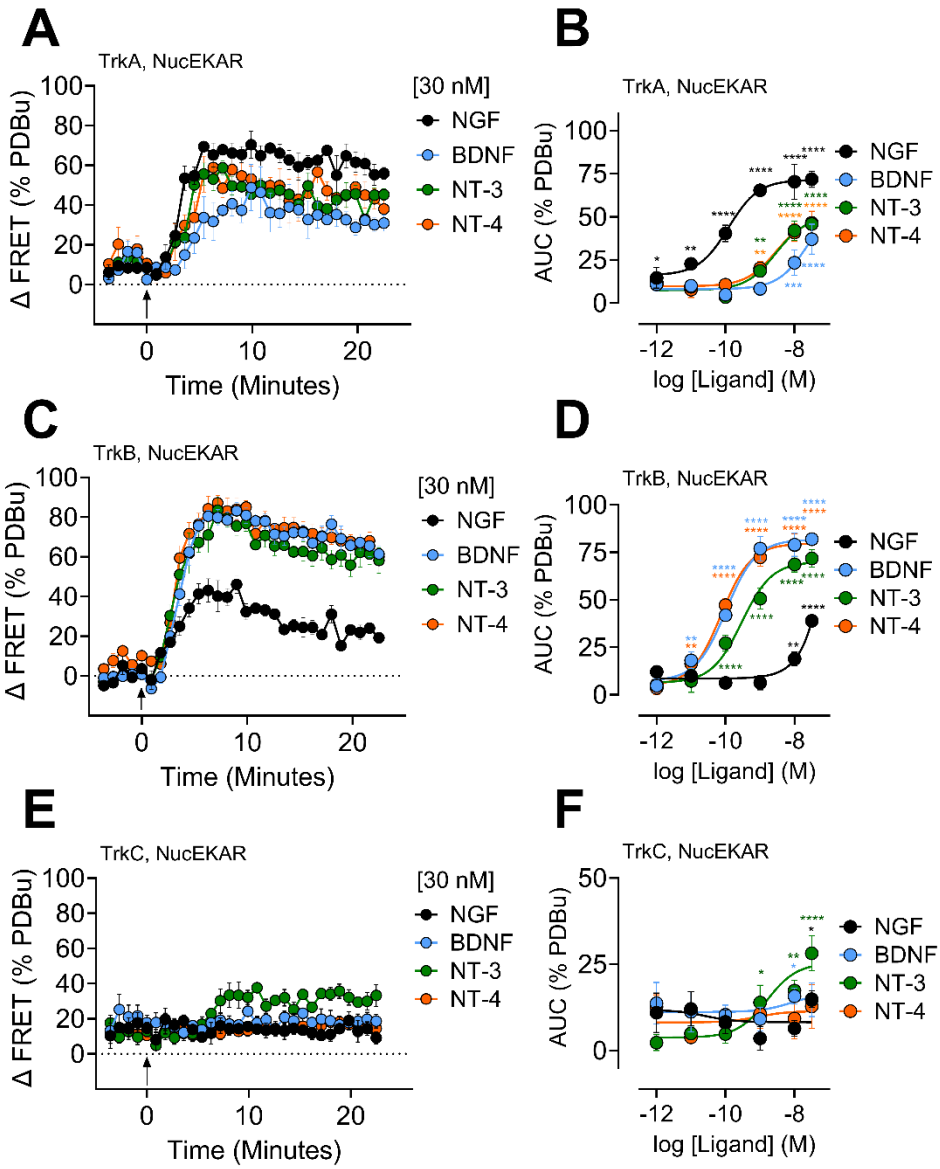


Figure 6. **TrkC had slower and reduced ERK signalling compared to TrkA or TrkB.** (A,C,E) ERK signalling was measured in response to 30 nM of each neurotropic growth factors. Data is expressed as change in FRET ratio over 25 minutes. (B,D,F) Concentration-response data obtained from the corresponding kinetic graph (Fig.5B-E) calculated as area under the (AUC). Data expressed as as a percentage of vehicle (0%) and 10 μM PDBu (100%). Mean ± SEM, from 4-5 independent experiments with triplicate wells. Derived potency values and kinetic values are provided in Table 3. Significance (B,D,F) was determined using ordinary two-way ANOVA with Dunnett's multiple comparisons test versus vehicle. Statistical significance denoted as p<0.05 (*), p<0.01 (**), p<0.001 (***), and p<0.0001 (****).

Tables & Table Legends

Table 1: **Summary of potency (pEC_{50}) and kinetic (k_{obs}) values derived for Trk dimerisation**. Data are presented as mean ± SEM from 5 independent replicates with triplicate wells. K_{obs} values were derived from Trk dimerisation in response to 30 nM ligand. 'Not determined' (ND) indicates the response was insufficient to generate a pEC_{50} or K_{obs} value.

	TrkA		**TrkB**		**TrkC**	
	pEC_{50}	K_{obs} (min^{-1})	pEC_{50}	K_{obs} (min^{-1})	pEC_{50}	K_{obs} (min^{-1})
NGF	8.88 ± 0.44	0.33 ± 0.04	ND	ND	ND	ND
BDNF	ND	ND	8.72 ± 0.24	0.56 ± 0.08	ND	0.35 ± 0.07
NT-3	8.99 ± 0.56	1.24 ± 0.57	8.59 ± 0.18	2.02 ± 0.64	8.70 ± 0.07	0.39 ± 0.03
NT-4	8.58 ± 0.34	0.86 ± 0.22	9.22 ± 0.10	0.86 ± 0.10	ND	ND

Table 2: **Summary of potency (pEC_{50}) and kinetic (k_{obs}) values derived for Trk trafficking**. Data are presented as mean ± SEM from 4-5 independent replicates with triplicate wells. K_{obs} values were derived from Trk trafficking in response to 30 nM ligand. 'Not determined' (ND) indicates the response was insufficient to generate a pEC_{50} or K_{obs} value.

	TrkA		**TrkB**		**TrkC**	
	pEC_{50}	K_{obs} (min^{-1})	pEC_{50}	K_{obs} (min^{-1})	pEC_{50}	K_{obs} (min^{-1})
NGF	9.02 ± 0.09	0.80 ± 0.40	8.05 ± 0.12	1.06 ± 0.54	ND	ND
BDNF	ND	ND	8.63 ± 0.43	0.30 ± 0.08	ND	ND
NT-3	7.83 ± 0.17	0.23 ± 0.02	8.48 ± 0.09	0.39 ± 0.05	9.35 ± 0.44	0.27 ± 0.05
NT-4	8.16 ± 0.08	0.36 ± 0.11	8.47 ± 0.18	0.31 ± 0.05	ND	ND

Table 3: **Summary of potency (pEC_{50}) and kinetic (k_{obs}) values derived for Trk nuclear ERK signalling**. Data are presented as mean ± SEM from 4-5 independent replicates with triplicate wells. While the pEC_{50} values are determined from the area under the curve, kinetic K_{obs} values were derived from between 2 & 15 minutes of the nuclear ERK signalling assay in response to 30 nM ligand**.** 'Not determined' (ND) indicates the response was insufficient to generate a pEC_{50} or K_{obs} value.

	TrkA		**TrkB**		**TrkC**	
	pEC_{50}	K_{obs} (min^{-1})	pEC_{50}	K_{obs} (min^{-1})	pEC_{50}	K_{obs} (min^{-1})
NGF	9.91 ± 0.09	2.54 ± 1.53	ND	1.22 ± 0.27	ND	ND
BDNF	ND	ND	9.95 ± 0.10	0.77 ± 0.21	ND	ND
NT-3	8.45 ± 0.14	1.14 ± 0.33	9.48 ± 0.18	1.32 ± 0.26	9.06 ± 0.25	0.14 ± 0.06
NT-4	8.50 ± 0.17	0.90 ± 0.25	10.20 ± 0.10	1.24 ± 0.09	ND	ND